

X-716-68-204

PREPRINT

NASA TM X-63272

PHOTOVOLTAIC PROPERTIES OF U.S. AND EUROPEAN SILICON CELLS UNDER 1-Mev ELECTRON IRRADIATION

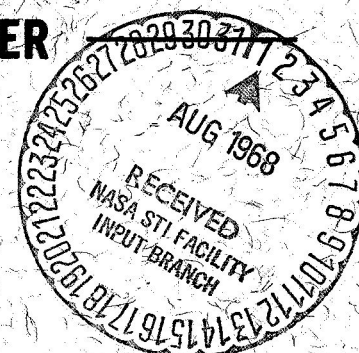
FACILITY FORM 602	N 68-29436	
	(ACCESSION NUMBER)	(THRU)
	26	1
	(PAGES)	(CODE)
	TMX-63272	03
	(NASA CR OR TMX OR AD NUMBER)	(CATEGORY)

WILLIAM R. CHERRY
RICHARD L. STATLER

APRIL 1968



GODDARD SPACE FLIGHT CENTER
GREENBELT, MARYLAND



X-716-68-204

PREPRINT

PHOTOVOLTAIC PROPERTIES OF U.S. AND
EUROPEAN SILICON CELLS UNDER
1-Mev ELECTRON IRRADIATION

William R. Cherry
Goddard Space Flight Center
Greenbelt, Maryland

and

Richard L. Statler
Naval Research Laboratory
Washington, D. C.

April 1968

GODDARD SPACE FLIGHT CENTER
Greenbelt, Maryland

ABSTRACT

This paper documents the procedures and results of a project to determine the electron radiation effects on silicon solar cells. Samples of U.S. and European cells were irradiated by means of Van de Graaff generators at Goddard Space Flight Center and the Naval Research Laboratory, and the I-V curves were determined to reveal the effects of the radiation. The paper also provides data on maximum power and power at 0.35 volt for each cell irradiated. Tests were conducted on specimens manufactured in 1966 and in 1967. The paper facilitates comparison of the various cells and their associated radiation effects by the inclusion of open-circuit voltage and short-circuit current data in tabular form.

CONTENTS

Abstract.....	ii
INTRODUCTION.....	1
EXPERIMENTAL PROCEDURE.....	1
RESULTS OF EXPERIMENT.....	4
CONCLUSIONS.....	10
ACKNOWLEDGMENTS.....	11

LIST OF ILLUSTRATIONS

<u>Figure</u>		<u>Page</u>
1	Solar Cell Irradiation Fixture.	11
2	Range of Performance of Commercially Available 10-ohm-cm N/P Silicon Cells (1966 and 1967)	12
3	Performance of AEG-Telefunken (German) Cells	12
4	Performance of Centralab Cells	13
5	Performance of Ferranti (British) Cells.	13
6	Performance of SAT (French) Cells.	14
7	Performance of Siemens (German) Cells	14
8	Performance of Heliotek-2 Cells.	15
9	Performance of Heliotek-10 Cells	15
10	Performance of Ion Physics Cells	16
11	Performance of NASA-Lewis Cells	16
12	Performance of Texas Instruments Cells	17
13	Performance of Westinghouse Cells.	17
14	I-V Curves for AEG-Telefunken Cell A-10 (10 ohm-cm, Boron-Doped)	18
15	I-V Curves for AEG-Telefunken Cell A-9-A (10 ohm-cm, Aluminum-Doped).	18
16	I-V Curves for Centralab Cell C-10 (10 ohm-cm, Boron-Doped).	18
17	I-V Curves for Ferranti Cell B-10 (10 ohm-cm, Boron-Doped).	18
18	I-V Curves for SAT Cell F-9 (10 ohm-cm, Boron-Doped)	19
19	I-V Curves for Siemens Cell G-10 (10 ohm-cm, Boron-Doped).	19
20	I-V Curves for Heliotek Cell H-9-2 (2 ohm-cm, Boron-Doped).	19
21	I-V Curves for Heliotek Cell H-10 (10 ohm-cm, Boron-Doped).	19
22	I-V Curves for Ion Physics Cell I-10 (10 ohm-cm, Boron-Doped)	20
23	I-V Curves for NASA-Lewis Cell L-10 (10 ohm-cm, Boron-Doped).	20

<u>Figure</u>		<u>Page</u>
24	I-V Curves for NASA-Lewis Cell L-10-A (10 ohm-cm, Aluminum-Doped)	20
25	I-V Curves for Texas Instruments Cell T-10 (10 ohm-cm, Boron-Doped)	20
26	I-V Curves for Texas Instruments Cell T-10-A (10 ohm-cm, Aluminum-Doped) . .	21
27	I-V Curves for Westinghouse Cell W-9 (Drift Field)	21

LIST OF TABLES

<u>Table</u>		<u>Page</u>
1	Cells Used in 1966 and 1967 Radiation Damage Study	2
2	Comparison of I_{sc} Between NRL and GSFC X25L Simulators	2
3	Radiation Exposure Schedule	3
4	V_{oc} in Millivolts Versus 1-Mev Electron Dose	6
5	I_{sc} in Milliamperes Versus 1-Mev Electron Dose	6
6	P_{max} Efficiency (%) Versus 1-Mev Electron Dose.	7
7	$P_{0.35v}$ Efficiency (%) Versus 1-Mev Electron Dose.	8
8	Average Solar Cell Parameters for 1-Mev Electron Radiation	8

PHOTOVOLTAIC PROPERTIES OF U.S. AND
EUROPEAN SILICON CELLS UNDER
1-Mev ELECTRON IRRADIATION

by
William R. Cherry
Goddard Space Flight Center

and
Richard L. Statler
Naval Research Laboratory

INTRODUCTION

Samples of silicon solar cells were obtained from various producers in the United States and Europe about midyear 1966 and 1967 (see Table 1). Specimens from Germany, Great Britain, and France were included as well as standard production U.S. cells, ion-implanted junction, webbed-dendrite, drift field, and three sets of boron and aluminum base-doped devices. Maximum power, power at 0.35v, and typical I-V curves for each source are shown in the report. Open-circuit voltages and short-circuit currents are presented in tabular form to allow comparison of cells. A transparent overlay showing the maximum power and power at 0.35v of standard U.S. production solar cells as a function of 1-Mev electron fluence is provided for the convenience of the reader. It can be used to compare the relative degradation of one cell to another. It should be noted that cells used in this study were not obtained by a random sampling process, but may have been selected carefully and matched by the producer.

EXPERIMENTAL PROCEDURE

The I-V curve for each solar cell was obtained before irradiation by a Spectrolab X-25L solar simulator. The 1967 data were obtained using an X-25L at the Naval Research Laboratory (NRL), and the 1966 data were obtained under the same intensity and temperature conditions using an X-25L at the Goddard Space Flight Center. The intensity of the two simulators was adjusted to 140 mw/cm² using a JPL balloon-flight standard cell for calibration. Further comparison of the two light sources was made by measuring the I-V curves of the group of 10 Heliotek 10-ohm-cm N/P cells from the 1966 experiment on the two light sources just before the 1967 experiment. This comparison is shown in Table 2. The cells were measured in a water-cooled cell holder at a temperature of 26°C, using 4-terminal pressure contacts to eliminate contact resistance effects

Table 1

Cells Used in 1966 and 1967 Radiation Damage Study.

Source	Year	Cell Type
Centralab (Hoffman)	1966-67	10-ohm-cm N/P boron
Heliotek	1966-67	10-ohm-cm N/P boron
Heliotek	1967	2-ohm-cm N/P boron
Texas Instruments	1966-67	10-ohm-cm-N/P boron
	1967	10-ohm-cm N/P aluminum
Ion Physics	1966-67	10-ohm-cm N/P ion implanted
Westinghouse	1966	10-ohm-cm N/P webbed dendrite
	1967	10-ohm-cm N/P webbed-dendrite, drift field
NASA-Lewis	1967	10-ohm-cm N/P boron
	1967	10-ohm-cm N/P aluminum
Ferranti (British)	1966-67	10-ohm-cm N/P boron
SAT (French)	1966-67	10-ohm-cm N/P boron
Siemens (German)	1966	1-ohm-cm N/P boron
	1967	10-ohm-cm N/P boron
AEG-Telefunken (German)	1967	10-ohm-cm N/P boron
	1967	10-ohm-cm N/P aluminum

Table 2

Comparison of I_{sc} Between NRL and GSFC X-25L Simulators.
 (I_{sc} measured under X-25L at 140 mw/cm²)

Cell No.	Dosage (e/cm ²)	I_{sc} (ma) NRL	I_{sc} (ma) GSFC
HE-1	0	70.1	70.1
HE-2	0	70.6	70.5
HE-3	10 ¹³	70.7	71.0
HE-4	10 ¹³	70.7	69.8
HE-5	10 ¹⁴	68.7	67.2
HE-6	10 ¹⁴	69.1	67.7
HE-7	10 ¹⁵	62.3	61.0
HE-8	10 ¹⁵	63.1	61.2
HE-9	10 ¹⁶	52.3	50.5
HE-10	10 ¹⁶	53.7	51.2
Average I_{sc} for Each Dosage at Different Simulators			
Percentage Difference (%)	Dosage (e/cm ²)	NRL (ma)	GSFC (ma)
<0.1	0	70.4	70.3
0.4	10 ¹³	70.7	70.4
2.0	10 ¹⁴	68.9	67.5
2.5	10 ¹⁵	62.7	61.1
4.0	10 ¹⁶	53.0	50.9

from the I-V curve. The intensity of the simulator was monitored continuously by means of the standard cell and displayed on a digital voltmeter throughout the measurement period.

The I-V curves were then plotted automatically on an X-Y recorder while a continuously variable resistive load was placed across the solar cell current terminals. These data were used to calculate efficiency, maximum output power, and power at a fixed voltage of 0.35 volt. The cells were then irradiated according to the schedule in Table 3. Following each incremental dosage, the I-V curve for each irradiated cell was obtained under the calibrated solar simulator.

Table 3
Radiation Exposure Schedule.

Dose	Dose Rate (e/cm ² /sec)	No. of I-V Measurements Taken at Each Dose Level for Each Cell Source		No. of Cells Withdrawn at Dose Level	
		1966	1967	1966	1967
0	0	10	10	2	2
10 ¹³	10 ¹⁰	8	8	2	2
10 ¹⁴	10 ¹¹	6	6	2	2
10 ¹⁵	2 × 10 ¹¹	4	4	2	1
5 × 10 ¹⁵	4 × 10 ¹¹	--	3	--	1
10 ¹⁶	4 × 10 ¹¹	2	2	2	2

The bombardment of the 1967 cells was done at the NRL 2-Mev electron Van de Graaff accelerator. This machine produces a vertical electron beam which is scattered through the 3-mil aluminum window and a 6-inch air path. The cumulative scattering effects of the window and air provide a beam spot with a 2-inch diameter and a 5-percent intensity variation as measured by a Faraday cup.

For dosage uniformity, all cells were placed in recesses near the periphery of an aluminum wheel (27.5-inch diameter) which was rotated at 10 rpm 6 inches below the beam tube of the Van de Graaff generator (Figure 1). Each cell thus moved in a circular path through the flux pattern at 6 inches below the exit window. This technique, together with the inherent beam current stability of the NRL 2-Mev Van de Graaff generator, ensured that all cells received the same exposure dosage to a fraction of 1 percent. The electron flux was calibrated before each bombardment by means of a vacuum Faraday cup placed in the center of the flux pattern through which the cells would later move. The measured flux was then correlated with the short-circuit current generated in a heavily preirradiated solar cell (approximately 10¹⁷ e/cm²) by exposure to the same flux. This cell was fastened near the periphery of the aluminum wheel in such a manner that its short-circuit current and temperature, by means of a thermistor, could be monitored through commutator contacts to a station outside the Van de Graaff room. A pre-irradiated cell was used to ensure that the diffusion length of the radiation monitoring cell remained practically constant. The

use of the cell attached to the wheel permitted an irradiation duty cycle to be obtained before each bombardment and provide for continuous monitoring of the exposure flux during the actual bombardment. At no time during the irradiation did the solar cell temperature exceed 34°C.

The 1966 cells were irradiated at the GSFC 2-Mev Van de Graaff generator in a similar manner. Even though the GSFC accelerator has a horizontal beam, the experimental procedures were comparable. Typical dosage rates are shown in Table 3.

RESULTS OF EXPERIMENT

The transparent overlay, Figure 2, is the "envelope" of data obtained from U.S. commercially available cells from Centralab, Heliotek, and Texas Instruments (T.I.), ranging from 9.9 to 10.6 percent air mass zero (AM0) efficiency and irradiated with 1-Mev electrons. Comparison of Figure 2 with Figures 3 through 13 reveals the comparative performance of cells submitted from other sources. It should be remembered that cells from other than the commercial producers might be highly selective and therefore not representative of production cells from that source. The illustrated values show the maximum power output for both 1966 and 1967 cells and power at 0.35v for 1967 cells to a 1-Mev electron fluence of $10^{16}/\text{cm}^2$. No samples were obtained in 1966 for AEG-Telefunken and NASA-Lewis. However, substantial improvement in performance was seen in SAT, Ferranti, Siemens (however, note odd effect), Ion Physics, and Westinghouse from 1966 to 1967. Production cells (Centralab, Heliotek, and T.I.) seem quite comparable for both years. In all cells except the Westinghouse webbed-dendrite drift field, the maximum power point and power at 0.35v coincide almost at 10^{16} 1-Mev electrons. The Westinghouse cell seemed to have maximum power at a voltage slightly greater than 0.35 volt at 10^{16} 1-Mev electrons.

Efficiencies are based on 2 cm² areas. Since there were a variety of bus bar and grid line designs and most cells are now flat mounted rather than shingled, the total 2 cm² area was charged to each device. Some of the European cells (SAT, AEG, and Siemens) were 4 cm²; therefore, the power shown is based on half the total cell output. Also, the Ion Physics ion-implanted cells were covered with CeO₂ as an antireflective coating. Experience has shown that a cell using CeO₂ is less efficient than a similar cell using SiO in air. The opposite is true after applying cover glasses.* Since all tests were performed in this experiment with cells without cover glass, the Ion Physics cells do not appear as efficient as they may be with cover slips.

Three organizations submitted both boron and aluminum base-doped 10-ohm-cm cells (AEG-Telefunken, NASA-Lewis, and Texas Instruments, Inc.). From the data observed in this experiment, there seems to be no significant difference in the maximum power output between the aluminum and boron-doped cells of AEG and NASA-Lewis. Texas Instruments aluminum-doped cells appear slightly superior to their boron-doped cells from 10^{15} to 10^{16} 1-Mev electron doses. This difference is, however, quite small and may result from the small sample size of the experiment at these large doses. The authors believe that there is little, if any, difference between aluminum and boron base-doped cells from a radiation resistance standpoint.

*"Reflections on a Solar Cell," Implion News, 1(2), Ion Physics Corp.

Ion-implanted cells (Figure 10) which have CeO_2 antireflection coatings, had initial efficiencies of about 9.4 percent. At 10^{15} and 10^{16} 1-Mev electron doses, their performance looked as good as that of commercial solar cells with initial efficiencies of 10 percent.

Webbed-dendrite, drift field cells (Figure 13) from Westinghouse had initial efficiencies of 9.6 percent but required about three times the dose to reduce their power output to the same level as a 10-percent efficient 10-ohm-cm commercial cell at a dose of 10^{15} 1-Mev electrons. This was particularly surprising because the drift field cell had open-circuit voltage characteristics of a 1-ohm-cm device. Perhaps this is one way to obtain both higher voltage and good radiation resistance.

AEG-Telefunken, SAT, and Ferranti cells all appear to withstand 1-Mev electron irradiation better than the U.S. commercial cells. To reach the same maximum power level as the equivalent U.S. cell at 10^{15} 1-Mev electrons, it was necessary to subject the European cells to two or more times as large a dose. While the European processes appeared to be very similar to U.S. methods, all of the previously mentioned sources used European silicon, as was explained to one of the authors on a 1967 tour of the European industry.

An unexplained effect was observed with the 1967 Siemens solar cells. They behaved in a normal manner as 10-ohm-cm cells up to a dose of 10^{14} 1-Mev electrons (Figure 7). Then the cells dropped into catastrophic decline at 10^{15} , 5×10^{15} and 10^{16} fluence. Measurements a few days after the irradiation showed some room-temperature annealing. Within 1 month, the highly damaged cells had recovered to the level of normal cells irradiated to the same degree. This strange effect is noted on the Siemens chart as solid and dotted circles. The 1967 curves for P_{max} and $P_{0.35\text{v}}$ are drawn through points measured 4 months after the irradiation. Cells submitted by Siemens in 1966 were very early state-of-the-art for them and had the properties of 1- to 2-ohm-cm silicon.

Figures 14 through 27 are I-V curves of typical cells received from each source. It should be noted, however, that the AEG aluminum, Ion Physics ion-implanted, and the NASA-Lewis boron curves shown are slightly better than the average of the cells tested while the Heliotek 2-ohm-cm cell and the Westinghouse webbed-dendrite, drift field I-V curves shown are slightly worse than the average. The rest of the I-V curves are typical of the samples measured.

Table 4 shows the average V_{oc} for each 1967 source of cells at the various dosages. By reference to Table 3 it will be seen that each figure appearing in the zero-dose column is the average of 10 cells, while the figure in the 10^{15} column is the average of 4 cells, etc. Notice that the Westinghouse webbed-dendrite, drift field cell developed voltages similar to, or higher than, the Heliotek 2-ohm-cm cells. The rest of the cells ranged from 538 mv to 551 mv, characteristic of 10-ohm-cm cells.

Table 5 shows the I_{sc} per 2 cm^2 for each source of cells at the various dose levels. The same number of measurements apply at each dose level as in the V_{oc} case and as shown in Table 3.

Table 4

 V_{oc} in Millivolts Versus 1-Mev Electron Dose.

Identification	0	10^{13} e/cm ²	10^{14} e/cm ²	10^{15} e/cm ²	5×10^{15} e/cm ²	10^{16} e/cm ²
AEG-boron	549	545	534	505	479	466
AEG-aluminum	550	548	535	507	481	470
Centralab-boron	548	544	525	493	468	456
Ferranti-boron	546	542	530	503	480	469
SAT-boron	543	541	531	502	479	468
Siemens-boron	551	549	530	499	472	459
Heliotek-boron-2	577	573	554	521	496	481
Heliotek-boron-10	544	540	523	492	466	455
Ion Physics-ion impl.	538	536	525	496	469	459
Lewis-boron	542	540	529	502	478	466
Lewis-aluminum	543	540	529	501	477	465
T.I.-boron	546	542	527	494	469	456
T.I.-aluminum	550	549	536	506	479	466
Westinghouse web/drift	592	590	580	542	501	482

Table 5

 I_{sc} in Milliamperes Versus 1-Mev Electron Dose.

Identification	0	10^{13} e/cm ²	10^{14} e/cm ²	10^{15} e/cm ²	5×10^{15} e/cm ²	10^{16} e/cm ²
AEG-boron	73.4	72.9	70.4	63.2	56.8	54.1
AEG-aluminum	71.6	71.3	68.6	61.4	54.5	52.5
Centralab-boron	68.3	67.8	64.1	57.0	51.0	47.8
Ferranti-boron	69.9	69.6	67.0	60.4	55.5	53.3
SAT-boron	68.8	68.2	66.3	60.1	54.5	52.4
Siemens-boron	72.1	71.5	67.8	59.6	52.5	49.7
Heliotek-boron-2	66.8	66.1	61.7	54.8	47.3	43.7
Heliotek-boron-10	71.1	70.9	67.5	60.2	53.9	51.3
Ion Physics-ion impl.	69.0	68.8	66.3	60.2	53.7	50.3
Lewis-boron	68.9	68.5	66.2	59.7	53.5	50.9
Lewis-aluminum	69.6	69.3	66.7	60.7	54.5	51.7
T.I.-boron	72.4	72.4	69.5	60.9	53.8	50.1
T.I.-aluminum	70.9	70.8	68.6	62.2	56.2	53.2
Westinghouse-web/drift	62.5	62.2	61.2	58.2	53.0	50.8

Table 6 compares the maximum power efficiencies, per 2 cm^2 , for the cells from each source. Data taken immediately after irradiation are shown for all cells. In the case of Siemens, remeasurements were made over several days and weeks which revealed a room-temperature annealing process was taking place. Data are shown in Tables 6 and 7 for the Siemens cells both immediately after irradiation and about 4 months later. When comparing with the AEG cells, it can be seen that recovery was nearly back to normal for the particular radiation dose which actually occurred in 1 month. Although cells from other sources were remeasured, even as long as 18 months after irradiation, less than 2 percent annealing was observed.

Table 7 shows the power at 0.35v for all cells at each radiation level and also the readings observed for the Siemens cells 4 months after the irradiations. Table 8 reports the average solar cell parameters as measured just before and immediately after irradiation with the 1-Mev electrons.

Table 6

P_{max} Efficiency (%) Versus 1-Mev Electron Dose.

Identification	0	10^{13} e/cm^2	10^{14} e/cm^2	10^{15} e/cm^2	$5 \times 10^{15} \text{ e/cm}^2$	10^{16} e/cm^2
AEG-boron	10.6	10.4	9.7	8.2	6.9	6.3
AEG-aluminum	10.5	10.4	9.6	8.1	6.8	6.3
Centralab-boron	10.0	9.8	8.8	7.3	6.2	5.6
Ferranti-boron	10.1	9.9	9.2	7.8	6.9	6.3
SAT-boron	9.9	9.7	9.1	7.9	6.7	6.2
Siemens-Immed. boron 4 mos.	10.7	10.5	9.4	6.0	4.3	3.8
	10.7	10.5	9.7	8.3	6.8	6.2
Heliotek-boron-2	10.3	10.1	9.1	7.6	6.1	5.5
Heliotek-boron-10	10.1	10.0	9.1	7.6	6.3	5.8
Ion Physics-ion impl.	9.4	9.3	8.7	7.4	6.1	5.6
Lewis-boron	9.6	9.5	8.9	7.6	6.5	6.0
Lewis-aluminum	9.7	9.6	9.0	7.6	6.4	5.8
T.I.-boron	9.9	9.8	9.0	7.4	6.2	5.6
T.I.-aluminum	9.6	9.6	9.0	7.7	6.6	6.0
Westinghouse-web/drift	9.5	9.5	9.1	8.2	6.9	6.2

Table 7

P_{0.35v} Efficiency (%) Versus 1-Mev Electron Dose.

Identification	0	10 ¹³ e/cm ²	10 ¹⁴ e/cm ²	10 ¹⁵ e/cm ²	5 × 10 ¹⁵ e/cm ²	10 ¹⁶ e/cm ²
AEG-boron	9.1	9.0	8.6	7.7	6.7	6.3
AEG-aluminum	8.9	8.8	8.5	7.5	6.6	6.2
Centralab-boron	8.4	8.4	7.9	6.9	6.0	5.6
Ferranti-boron	8.7	8.6	8.2	7.4	6.7	6.2
SAT-boron	8.5	8.4	8.2	7.4	6.5	6.1
Siemens-Immed. boron 4 mos.	9.0 9.0	8.9 8.9	8.4 8.7	5.9 7.6	3.7 6.7	2.9 6.1
Heliotek-boron-2	8.2	8.2	7.6	6.8	5.8	5.2
Heliotek-boron-10	8.7	8.7	8.3	7.2	6.3	5.8
Ion Physics-ion impl.	8.4	8.3	8.0	7.1	6.1	5.6
Lewis-boron	8.4	8.3	8.0	7.2	6.4	6.0
Lewis-aluminum	8.5	8.4	8.1	7.3	6.4	5.9
T.I.-boron	8.7	8.7	8.3	7.1	6.2	5.5
T.I.-aluminum	8.5	8.5	8.2	7.3	6.5	6.0
Westinghouse-web/drift	7.7	7.7	7.5	7.1	6.4	6.0

Table 8

Average Solar Cell Parameters for 1-Mev Electron Radiation.

Cell Type	1-Mev Electron Fluence (e/cm ²)	AM0 Efficiency (%)	Short- Circuit Current (ma)	Open- Circuit Voltage (mv)	Maximum Power (mw)	Power at 0.35 volt (mw)
AEG-Telefunken 10 ohm-cm, boron, 2 × 2 cm	0	10.6	146.8	549	59.4	50.7
	10 ¹³	10.4	145.9	545	58.5	50.3
	10 ¹⁴	9.7	140.9	534	54.3	48.4
	10 ¹⁵	8.2	126.3	505	45.9	43.1
	5 × 10 ¹⁵	6.9	113.5	479	38.7	37.6
	10 ¹⁶	6.3	108.2	466	35.4	35.4
AEG-Telefunken 10 ohm-cm, aluminum, 2 × 2 cm	0	10.5	143.2	550	58.9	49.7
	10 ¹³	10.4	142.7	548	58.2	49.2
	10 ¹⁴	9.6	137.3	535	53.7	47.5
	10 ¹⁵	8.1	122.9	507	45.6	42.2
	5 × 10 ¹⁵	6.8	109.1	481	38.1	36.8
	10 ¹⁶	6.3	105.0	470	35.2	34.8
Centralab 10 ohm-cm, boron, 1 × 2 cm	0	10.0	68.3	548	28.0	23.5
	10 ¹³	9.8	67.8	544	27.4	23.4
	10 ¹⁴	8.8	64.1	525	24.7	22.2
	10 ¹⁵	7.3	57.0	493	20.3	19.4
	5 × 10 ¹⁵	6.2	51.0	468	17.3	16.9
	10 ¹⁶	5.6	47.8	456	15.7	15.6

Table 8 (Continued)

Cell Type	1-Mev Electron Fluence (e/cm ²)	AM0 Efficiency (%)	Short- Circuit Current (ma)	Open- Circuit Voltage (mv)	Maximum Power (mw)	Power at 0.35 volt (mw)
Ferranti 10 ohm-cm, boron, 1 × 2 cm	0	10.1	69.9	546	28.3	24.3
	10 ¹³	9.9	69.6	542	27.7	24.1
	10 ¹⁴	9.2	67.0	530	25.8	23.1
	10 ¹⁵	7.8	60.4	503	21.8	20.7
	5 × 10 ¹⁵	6.9	55.5	480	19.4	18.7
	10 ¹⁶	6.3	53.3	469	17.5	17.4
Heliotek 10 ohm-cm, boron, 1 × 2 cm	0	10.1	71.1	544	28.3	24.5
	10 ¹³	10.0	70.9	540	28.0	24.4
	10 ¹⁴	9.1	67.5	523	25.4	23.1
	10 ¹⁵	7.6	60.2	492	21.2	20.3
	5 × 10 ¹⁵	6.3	53.9	466	17.7	17.6
	10 ¹⁶	5.8	51.3	455	16.3	16.3
Heliotek 2 ohm-cm, boron, 1 × 2 cm	0	10.3	66.8	577	28.8	23.0
	10 ¹³	10.1	66.1	573	28.4	22.9
	10 ¹⁴	9.1	61.7	554	25.6	21.4
	10 ¹⁵	7.6	54.8	521	21.4	18.9
	5 × 10 ¹⁵	6.1	47.3	496	17.1	16.1
	10 ¹⁶	5.5	43.7	481	15.4	14.7
SAT 10 ohm-cm, boron, 2 × 2 cm	0	9.9	137.5	543	55.6	47.7
	10 ¹³	9.7	136.5	541	54.4	47.0
	10 ¹⁴	9.1	132.6	531	51.2	45.6
	10 ¹⁵	7.9	120.3	502	43.9	41.2
	5 × 10 ¹⁵	6.7	109.1	479	37.4	36.5
	10 ¹⁶	6.2	104.9	468	34.9	34.4
Siemens 10 ohm-cm, boron, 2 × 2 cm	0	10.7	144.2	551	59.9	50.3
	10 ¹³	10.5	143.1	549	59.0	49.8
	10 ¹⁴	9.4	135.7	530	52.6	47.0
	10 ¹⁵	6.0	119.3	499	33.4	33.1
	5 × 10 ¹⁵	4.3	105.1	472	24.1	20.7
	10 ¹⁶	3.8	99.5	459	21.5	16.0
Westinghouse webbed- dendrite, drift field, boron, 1 × 2 cm	0	9.5	62.5	592	26.7	21.6
	10 ¹³	9.5	62.2	590	26.5	21.5
	10 ¹⁴	9.1	61.2	580	25.5	21.1
	10 ¹⁵	8.2	58.2	542	23.6	20.0
	5 × 10 ¹⁵	6.9	53.0	501	19.3	18.0
	10 ¹⁶	6.2	50.8	482	17.4	16.9
Ion Physics 10 ohm-cm, boron, 1 × 2 cm	0	9.4	69.0	538	26.2	23.4
	10 ¹³	9.3	68.8	536	26.0	23.3
	10 ¹⁴	8.7	66.3	525	24.3	22.4
	10 ¹⁵	7.4	60.2	496	20.8	20.0
	5 × 10 ¹⁵	6.1	53.7	469	17.2	17.1
	10 ¹⁶	5.6	50.3	459	15.7	15.7
NASA-Lewis 10 ohm-cm, boron, 1 × 2 cm	0	9.6	68.9	542	26.8	23.4
	10 ¹³	9.5	68.5	540	26.5	23.3
	10 ¹⁴	8.9	66.2	529	24.8	22.5
	10 ¹⁵	7.6	59.7	502	21.3	20.1
	5 × 10 ¹⁵	6.5	53.5	478	18.2	17.8
	10 ¹⁶	6.0	50.9	466	16.8	16.7

Table 8 (Continued)

Cell Type	1-Mev Electron Fluence (e/cm ²)	AM0 Efficiency (%)	Short- Circuit Current (ma)	Open- Circuit Voltage (mv)	Maximum Power (mw)	Power at 0.35 volt (mw)
NASA-Lewis 10 ohm-cm, aluminum, 1 × 2 cm	0	9.7	69.6	543	27.3	23.7
	10 ¹³	9.6	69.3	540	26.9	23.6
	10 ¹⁴	9.0	66.7	529	25.1	22.6
	10 ¹⁵	7.6	60.7	501	21.2	20.3
	5 × 10 ¹⁵	6.4	54.5	477	18.0	17.8
	10 ¹⁶	5.8	51.7	465	16.4	16.4
Texas Instruments 10 ohm-cm, boron, 1 × 2 cm	0	9.9	72.4	546	27.8	24.5
	10 ¹³	9.8	72.4	542	27.5	24.5
	10 ¹⁴	9.0	69.5	527	25.2	23.2
	10 ¹⁵	7.4	60.9	494	20.7	20.0
	5 × 10 ¹⁵	6.2	53.8	469	17.5	17.3
	10 ¹⁶	5.6	50.1	456	15.6	15.5
Texas Instruments 10 ohm-cm, aluminum, 1 × 2 cm	0	9.6	70.9	550	26.9	23.8
	10 ¹³	9.6	70.8	549	26.8	23.8
	10 ¹⁴	9.0	68.6	536	25.2	22.9
	10 ¹⁵	7.7	62.2	506	21.6	20.5
	5 × 10 ¹⁵	6.6	56.2	479	18.5	18.2
	10 ¹⁶	6.0	53.2	466	16.8	16.7

CONCLUSIONS

1. All 1967 European cells showed a marked improvement in efficiency over the samples submitted in 1966.

2. The average degradation of European 10-ohm-cm, boron-doped cells (excluding Siemens) was slightly less than the degradation of the three commercial U.S. 10-ohm-cm, boron-doped cells under equal 1-Mev electron doses. This is even true of the Siemens cells after a room-temperature annealing for at least 1 month. All of these cells used silicon obtained from European sources. The European cells required about 2×10^{15} 1-Mev electrons to reach the same level of degradation as U.S. commercial cells attain at 10^{15} e/cm².

3. Three producers provided both aluminum and boron-doped cells—AEG, NASA-Lewis, and T.I. No significant difference in performance was observed between the two types of doping in any case. Our conclusion is that it makes little difference in the room temperature degradation rates of 10-ohm-cm, silicon solar cells.

4. Initial efficiencies of both ion-implanted junction cells and webbed-dendrite, drift field cells appear approximately 5 percent lower than the average commercial N/P boron-doped diffused junction cell. However, at 10^{15} and 10^{16} electrons/cm² the ion-implanted cell was comparable with the commercial cells, while the webbed-dendrite, drift field maintained a higher power output, being approximately three times as radiation-resistant as the 10-ohm-cm N/P U.S. commercial cell. Some loss of performance in the ion-implanted cell may be attributed to the CeO₂ antireflection coating.

5. The observations made with respect to the Westinghouse webbed-dendrite, drift field cell are particularly interesting. It appears from these data that these cells have good resistance to radiation damage up to 10^{15} e/cm², at which dose the degradation rates increase substantially. In spite of these characteristics, however, the end-point efficiency was among the best of all cells examined. Also, their voltage remained high throughout the entire experiment.

6. As was expected, the degradation of 2-ohm-cm silicon cells was greater than for 10-ohm-cm cells with this difference becoming apparent at doses greater than 10^{15} e/cm² as determined by efficiency data.

7. The 1967 Siemens cell displayed unusually great degradation after 10^{14} e/cm². Periodic remeasurements showed a significant room-temperature annealing such that within 1 month the cells were comparable with other Western European cells. The cells had initial and final characteristics of 10-ohm-cm N/P solar cells. No explanation of this phenomenon has yet been made. Possibly low dose rates would not have affected this cell catastrophically at the higher doses, thus making it appear much more normal than under the high fluence rates of this experiment.

ACKNOWLEDGMENTS

Appreciation is expressed to the organizations which submitted solar cells for evaluation both in the U.S. and Europe. Particular thanks are due Messrs. William Gdula, Segun Park, and Jules Hirschfield of the Goddard Space Flight Center for assistance and support during the 1966 experiment and Mr. Max Sharp and personnel of Satellite Techniques Branch of the Naval Research Laboratory for similar help during 1967.

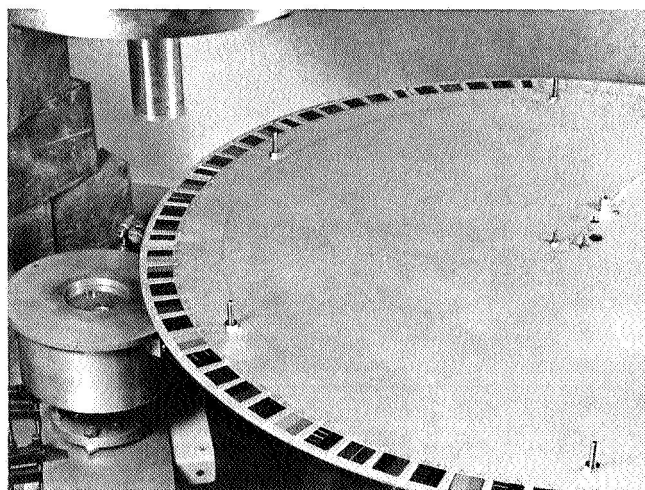


Figure 1—Solar Cell Irradiation Fixture.

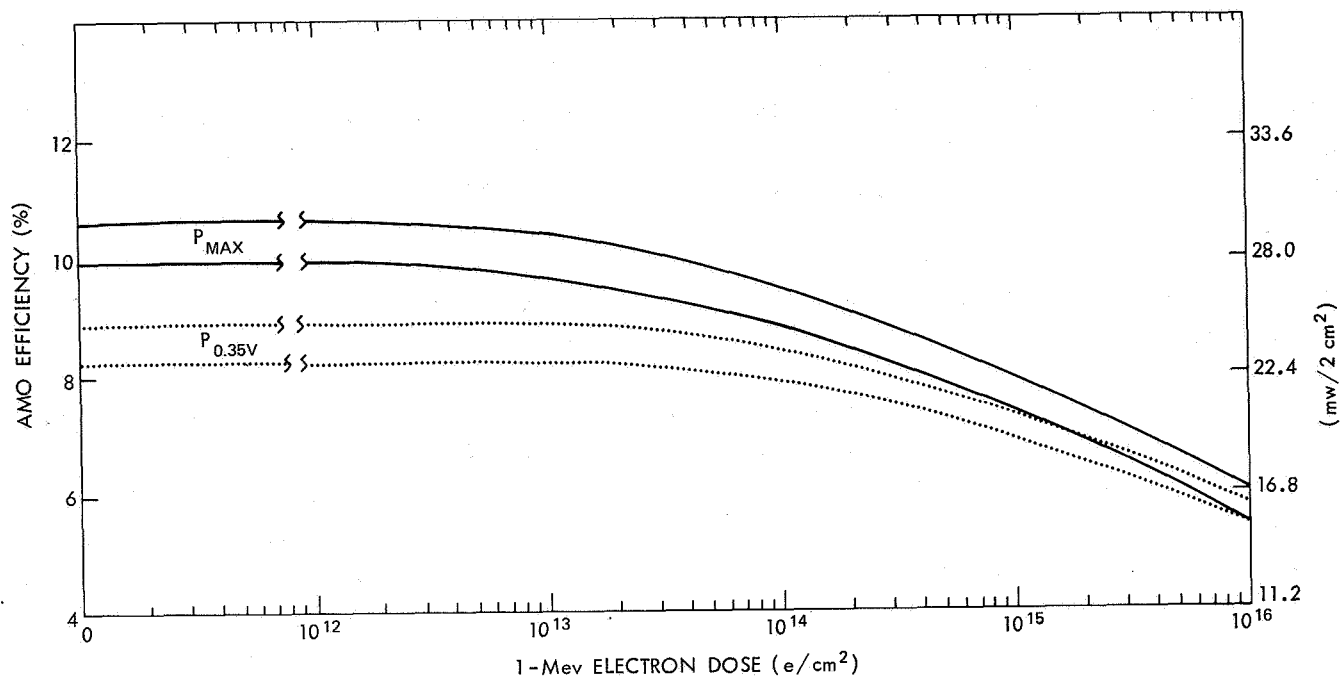


Figure 2—Range of Performance of Commercially Available 10-ohm-cm N/P Silicon Cells (1966 and 1967).

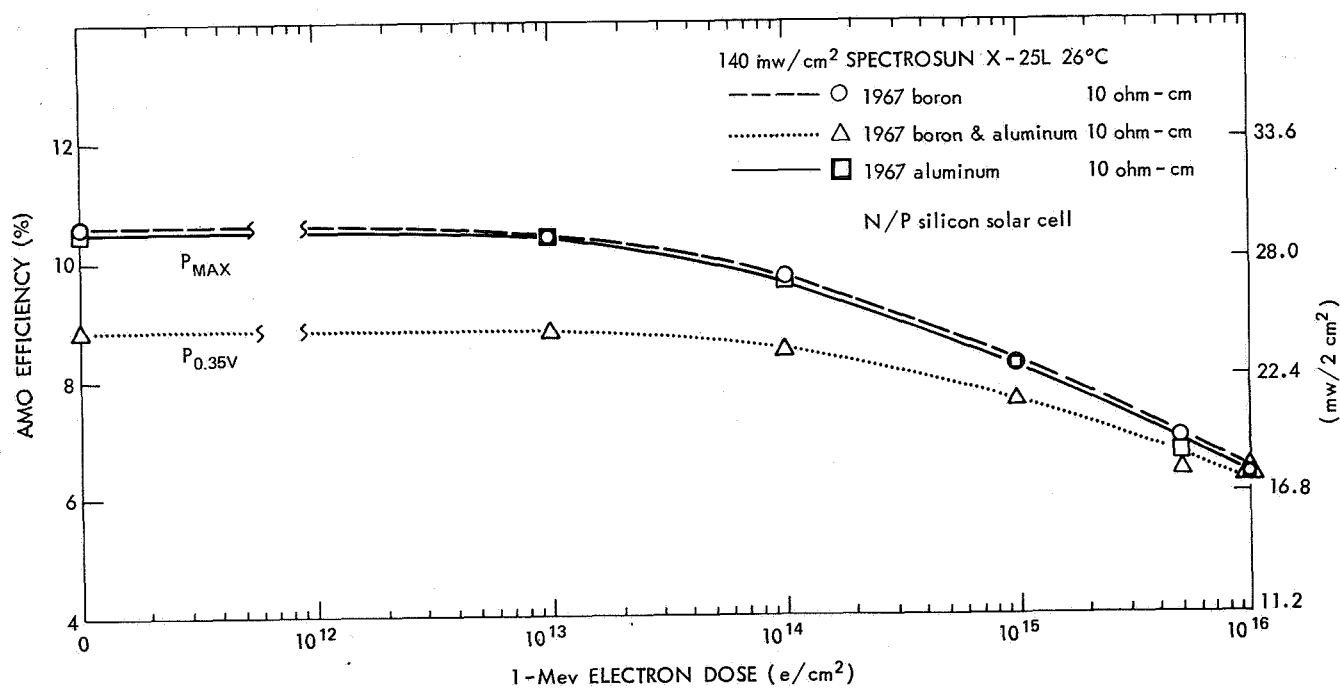


Figure 3—Performance of AEG-Telefunken (German) Cells.

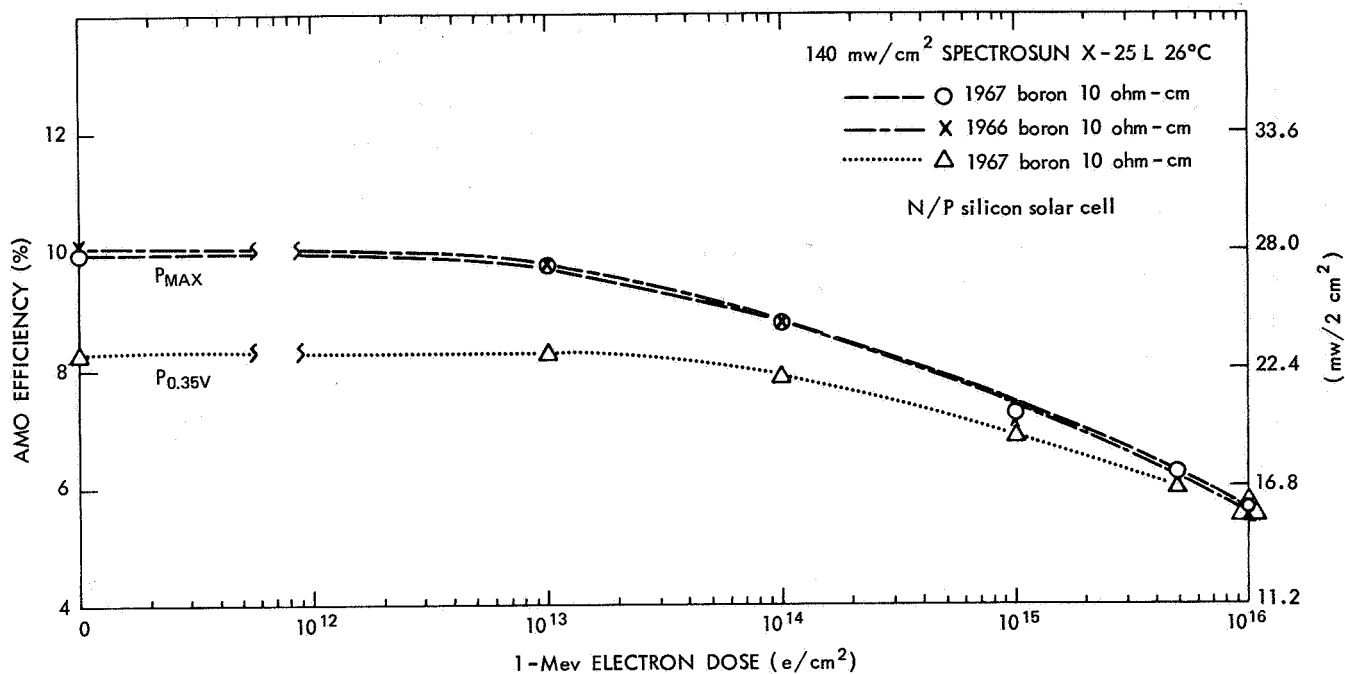


Figure 4—Performance of Centrallab Cells.

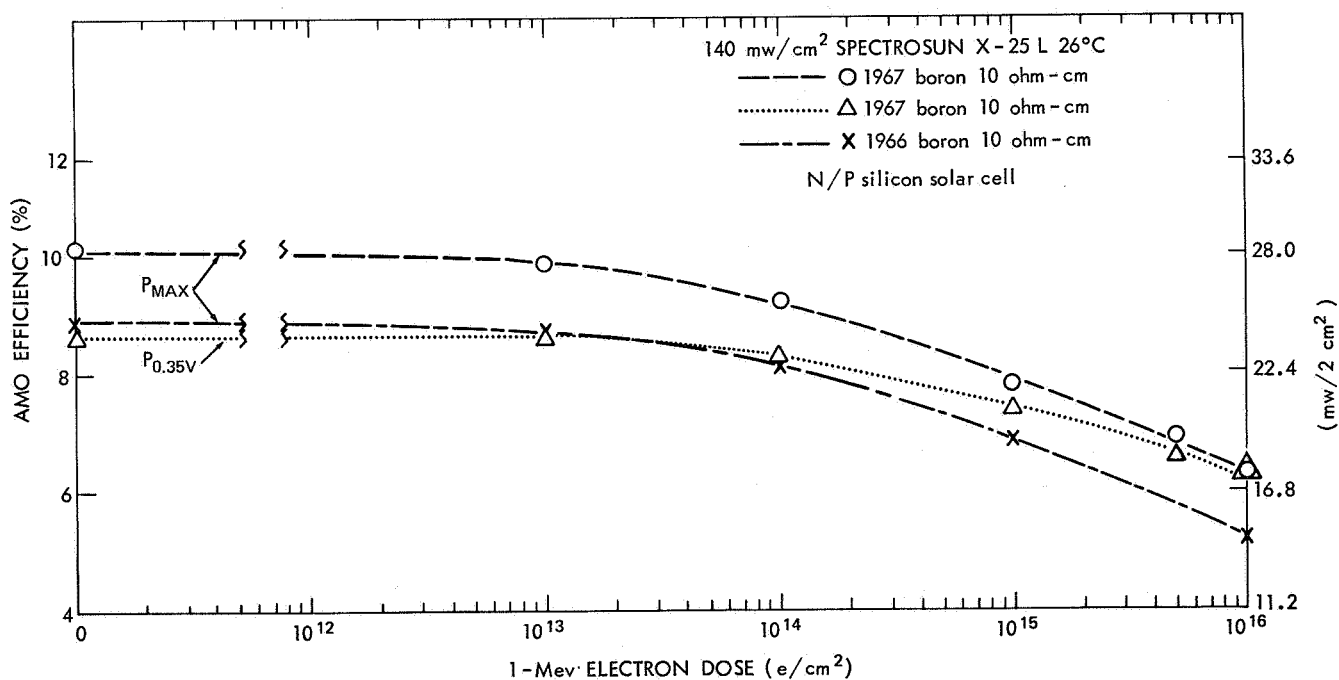


Figure 5—Performance of Ferranti (British) Cells.

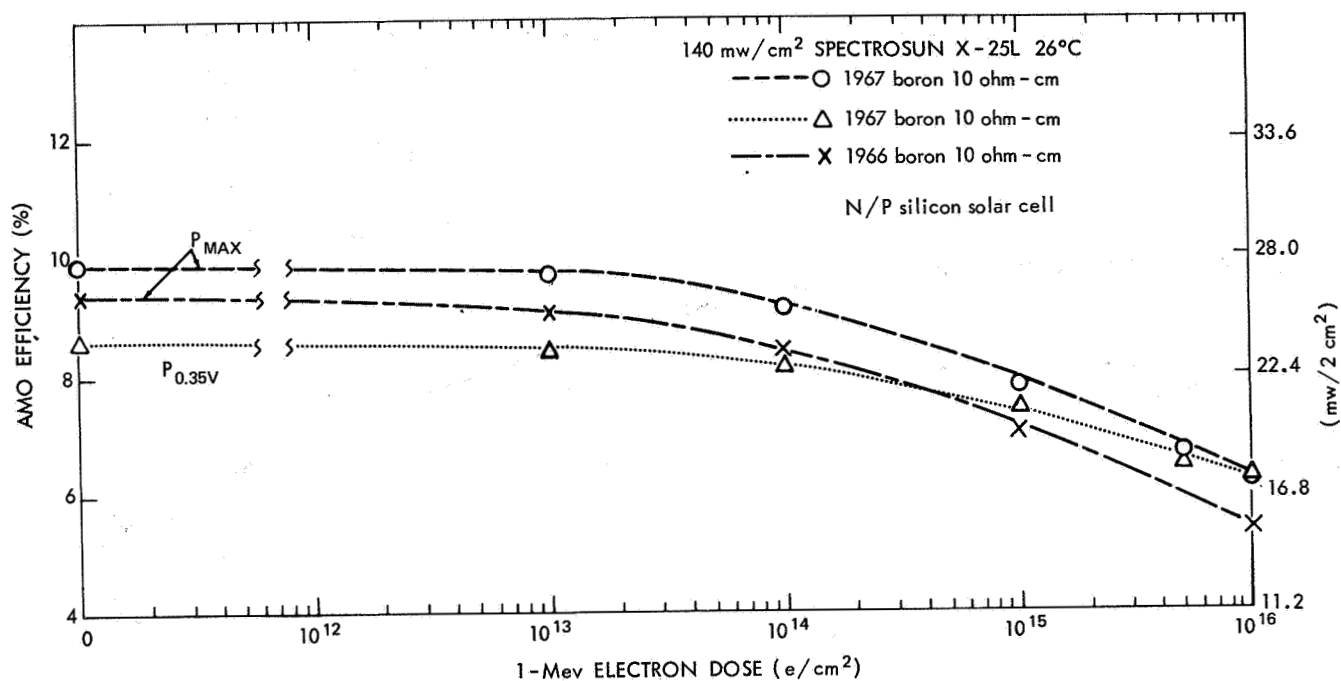


Figure 6—Performance of SAT (French) Cells.

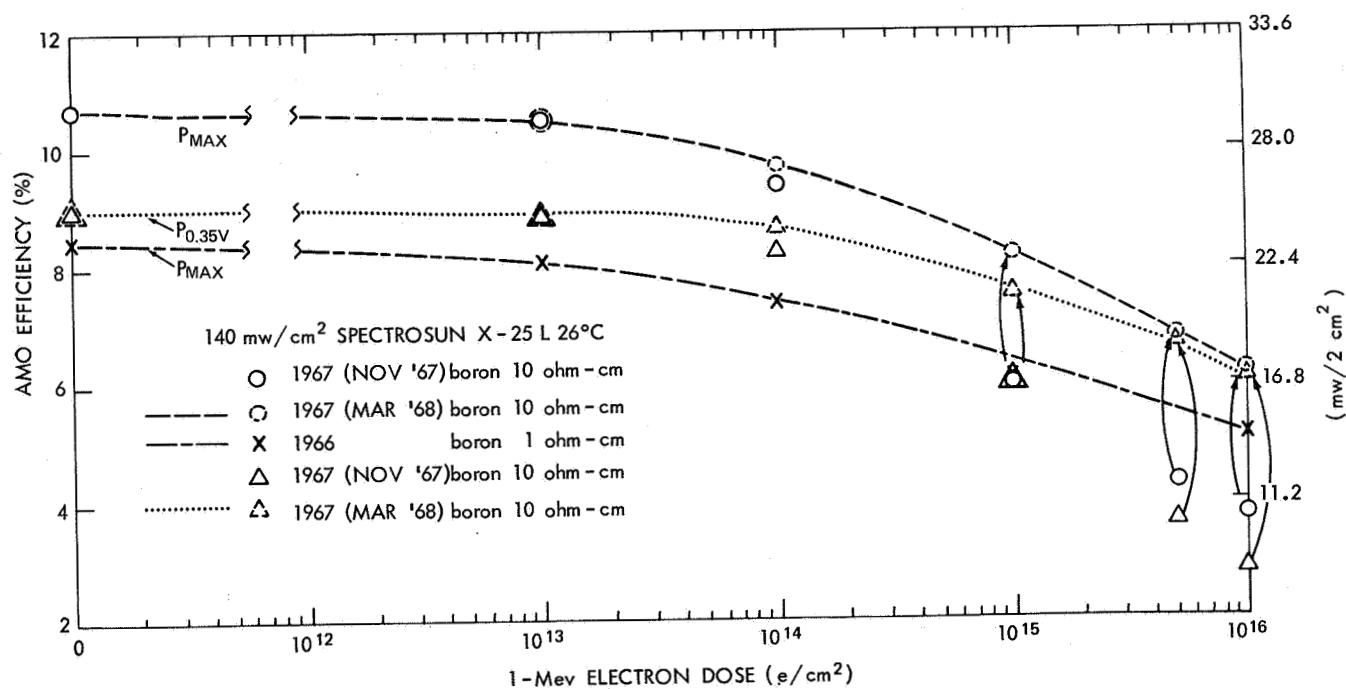


Figure 7—Performance of Siemens (German) Cells.

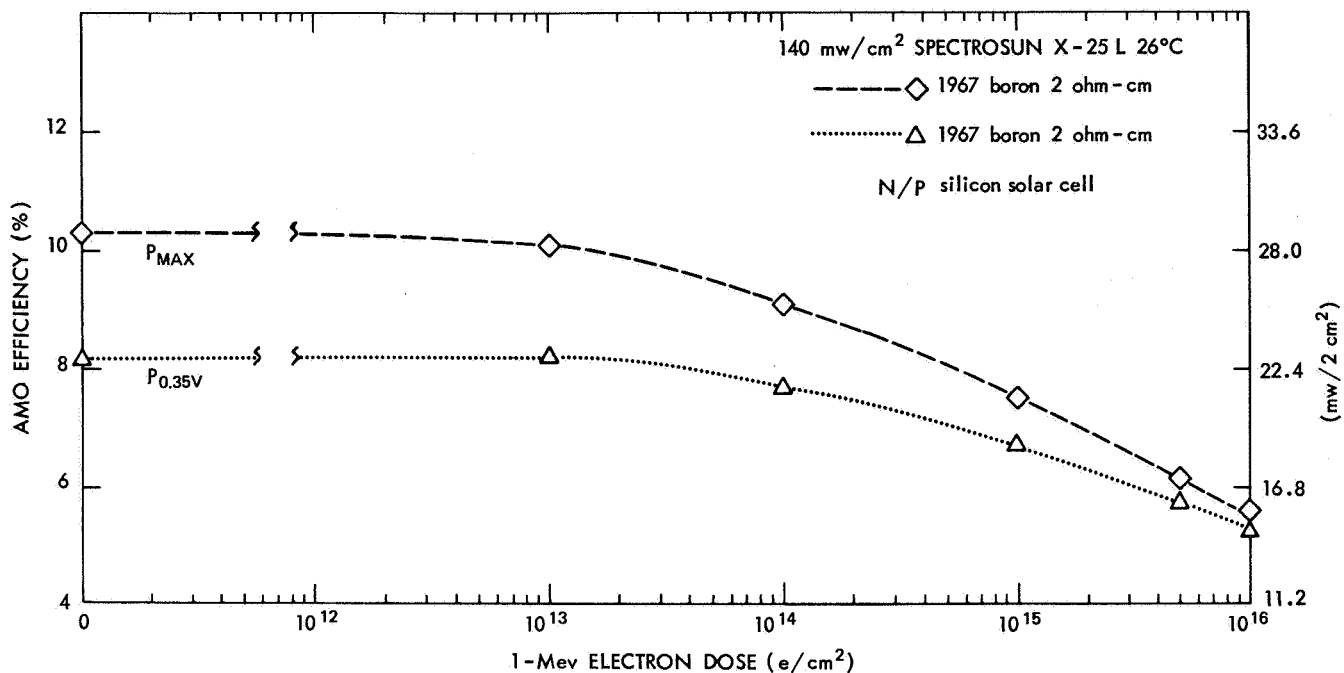


Figure 8—Performance of Heliotek-2 Cells.

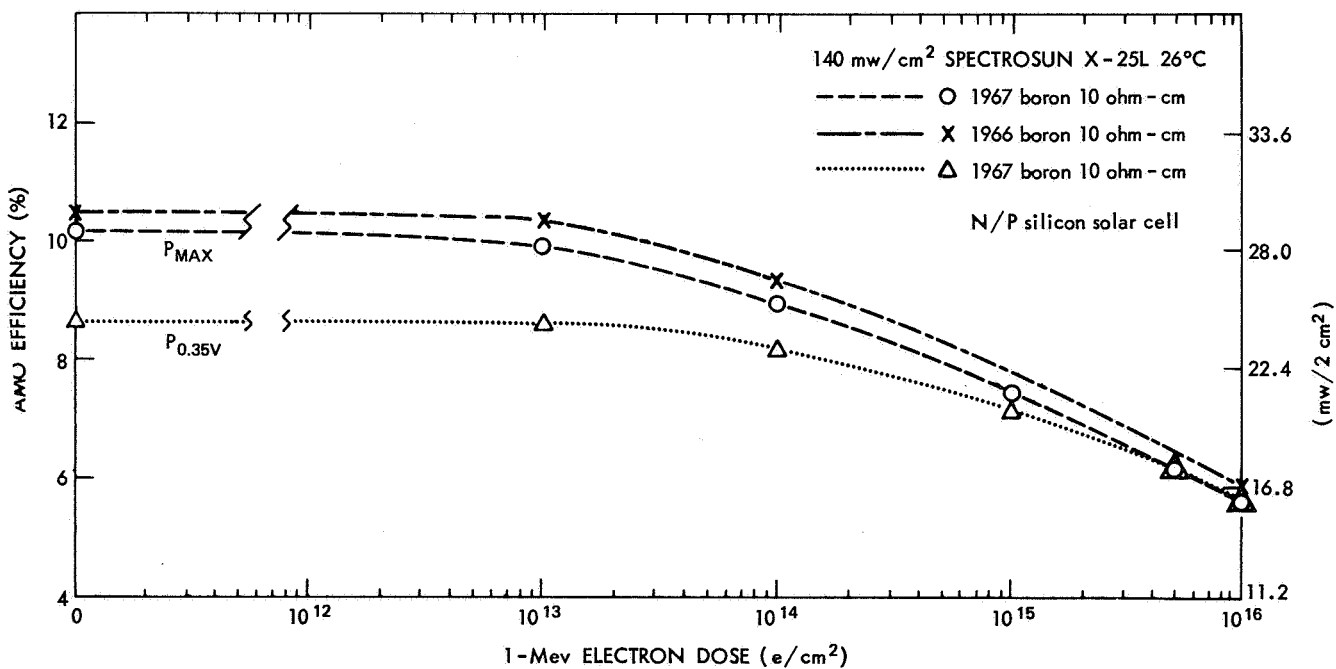


Figure 9—Performance of Heliotek-10 Cells.

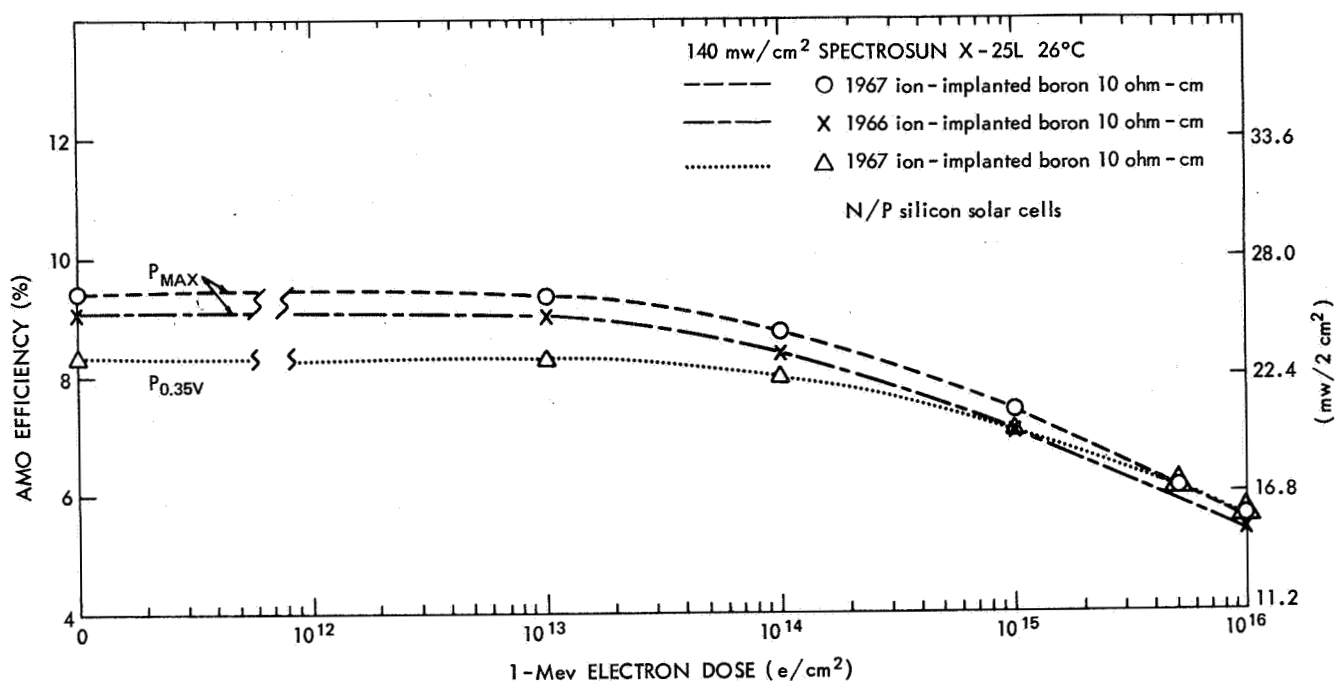


Figure 10—Performance of Ion Physics Cells.

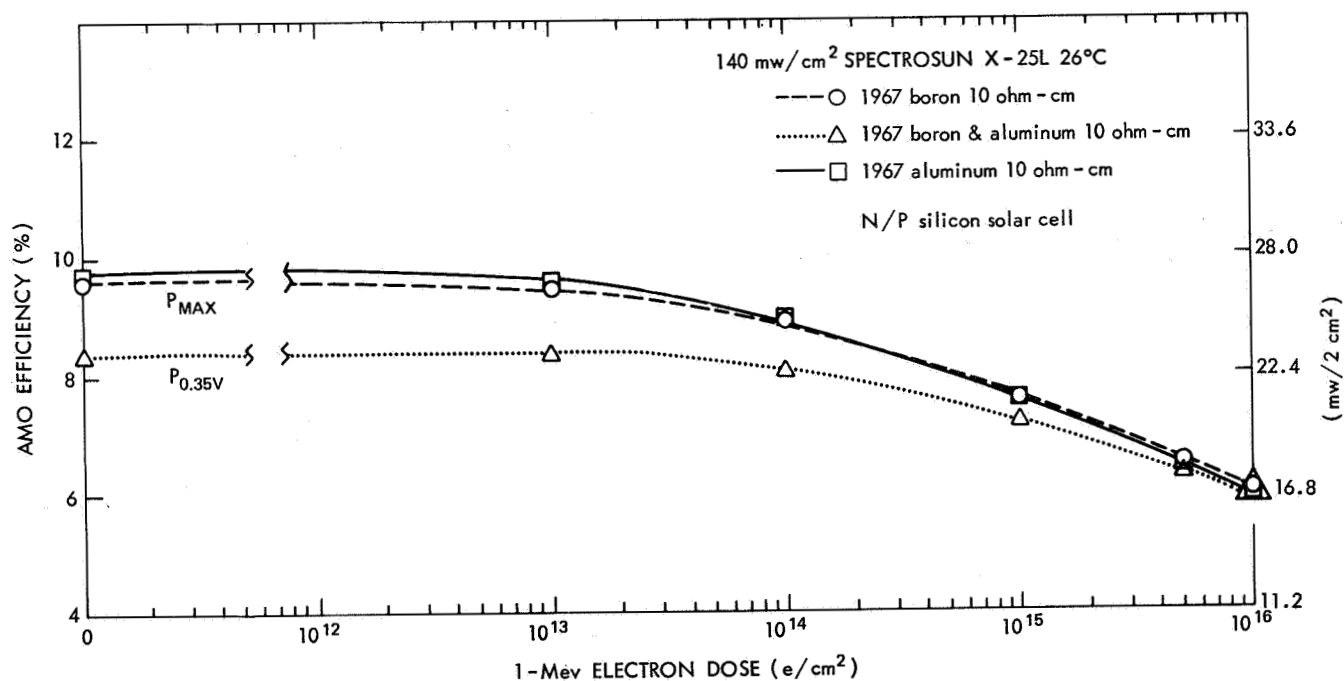


Figure 11—Performance of NASA-Lewis Cells.

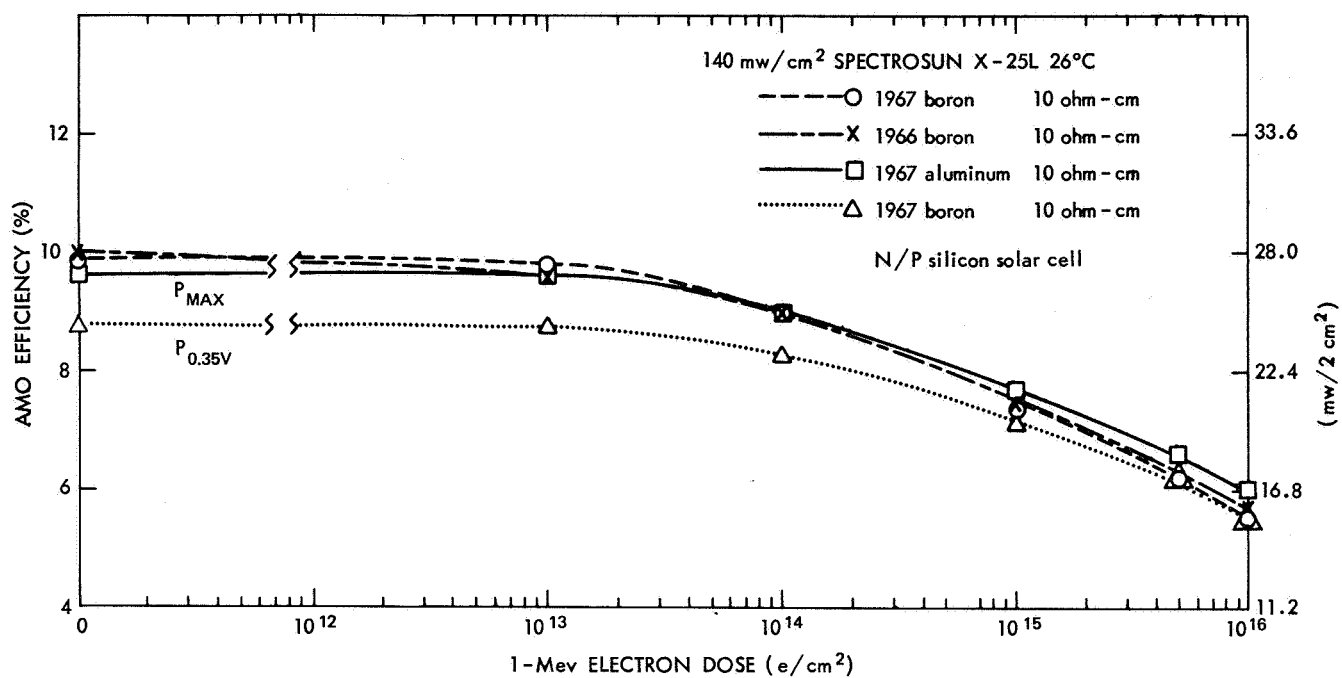


Figure 12—Performance of Texas Instruments Cells.

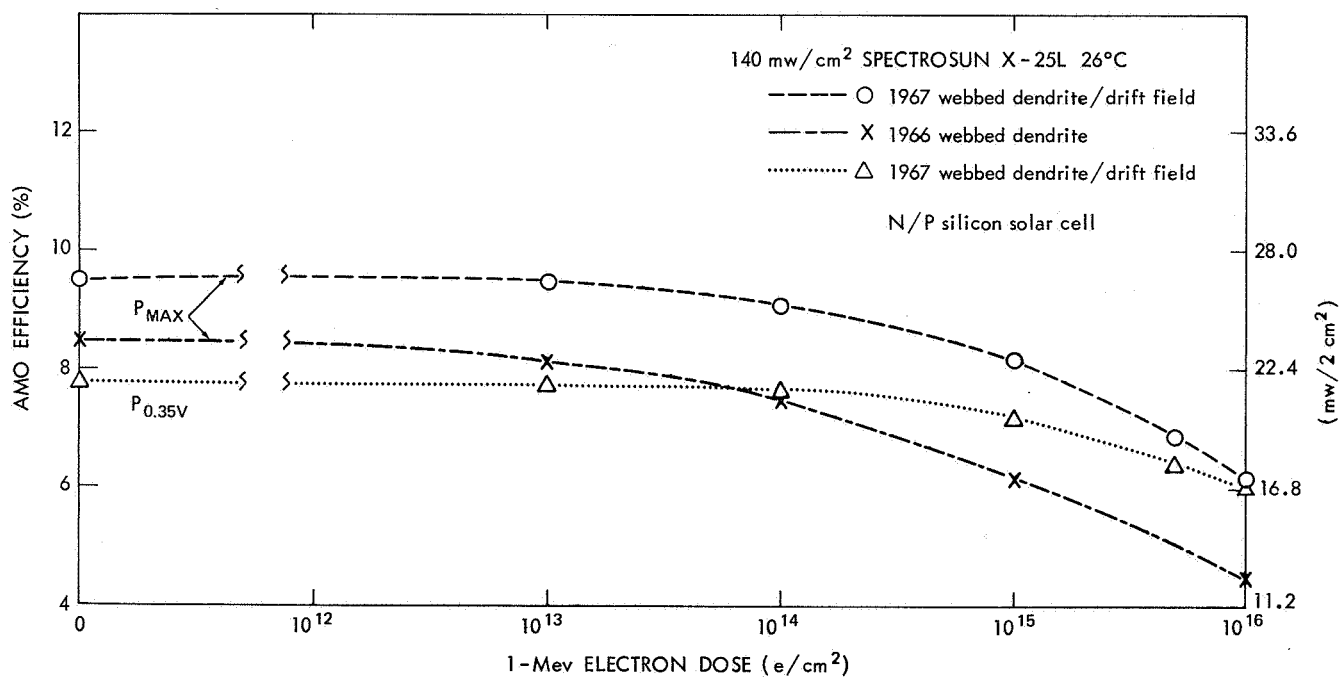


Figure 13—Performance of Westinghouse Cells.

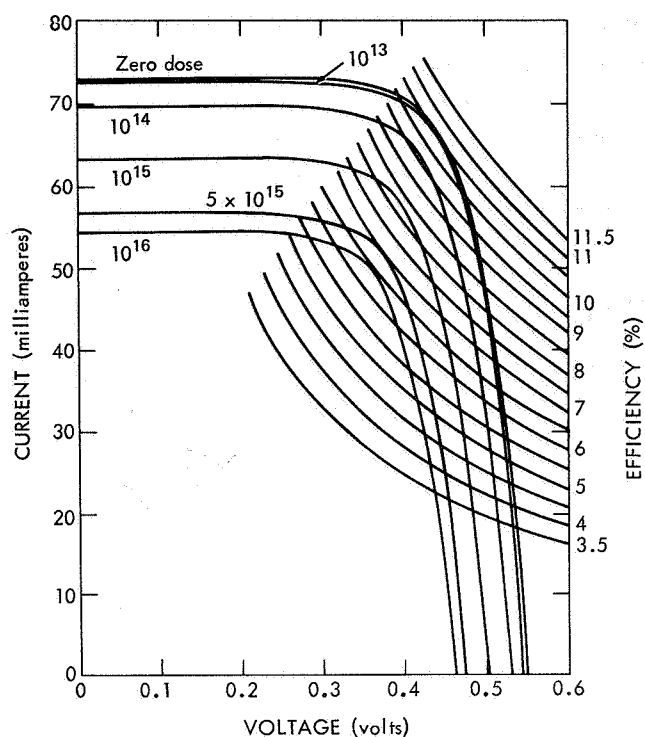


Figure 14—I-V Curves for AEG-Telefunken Cell A-10 (10 ohm-cm, Boron-Doped).

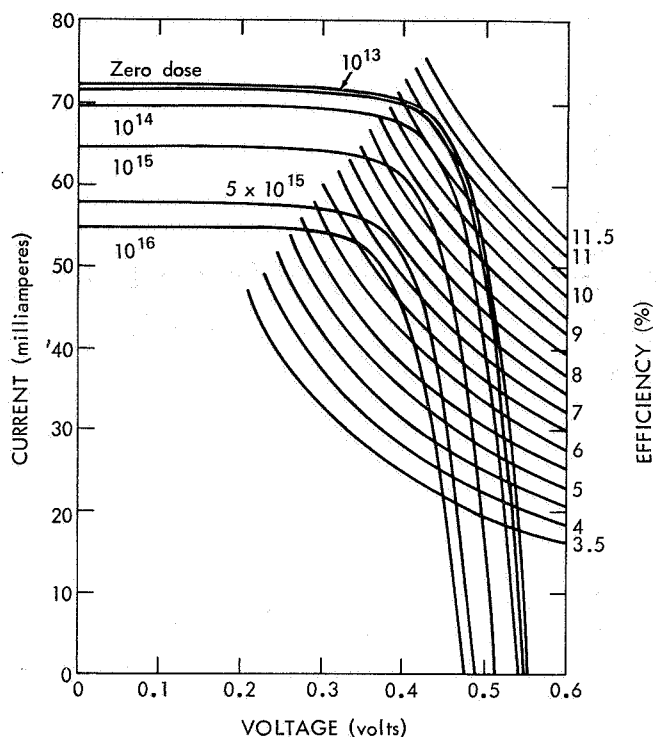


Figure 15—I-V Curves for AEG-Telefunken Cell A-9-A (10 ohm-cm, Aluminum-Doped).

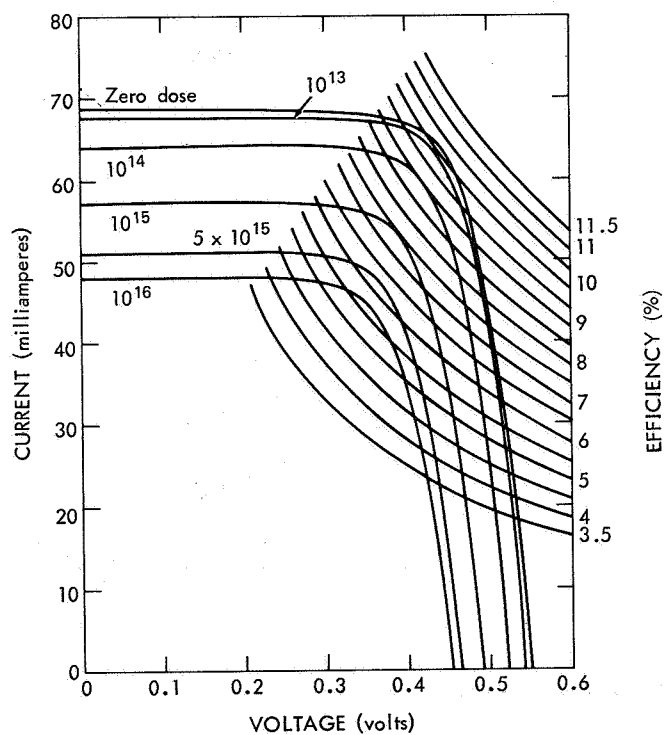


Figure 16—I-V Curves for Centralab Cell C-10 (10 ohm-cm, Boron-Doped).

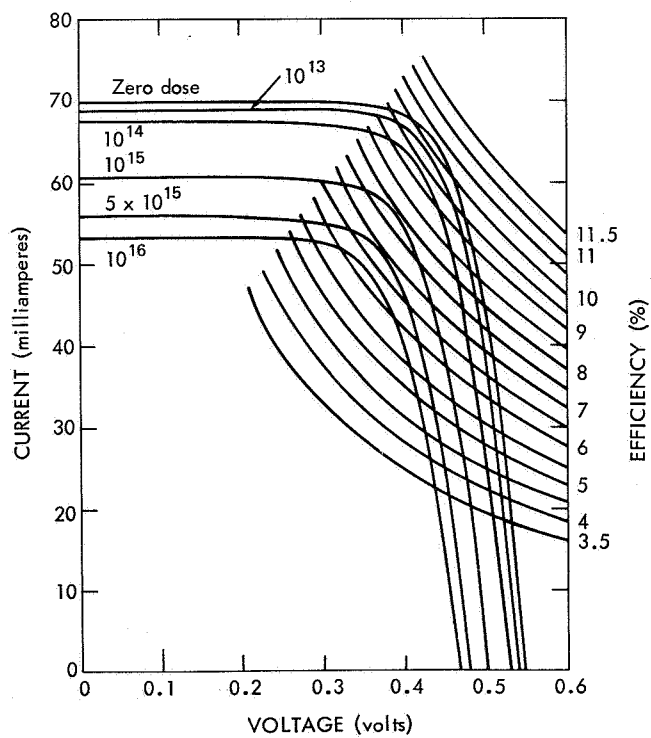


Figure 17—I-V Curves for Ferranti Cell B-10 (10 ohm-cm, Boron-Doped).

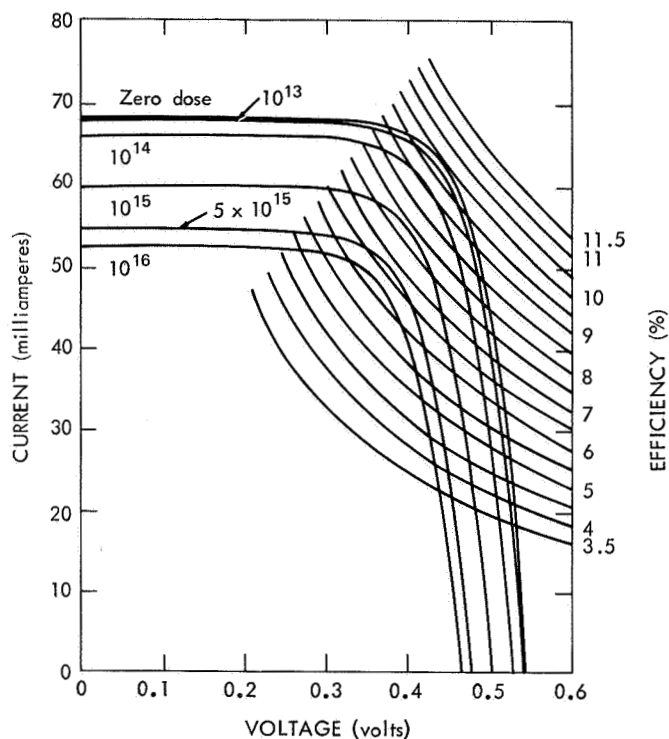


Figure 18—I-V Curves for SAT Cell F-9 (10 ohm-cm, Boron-Doped).

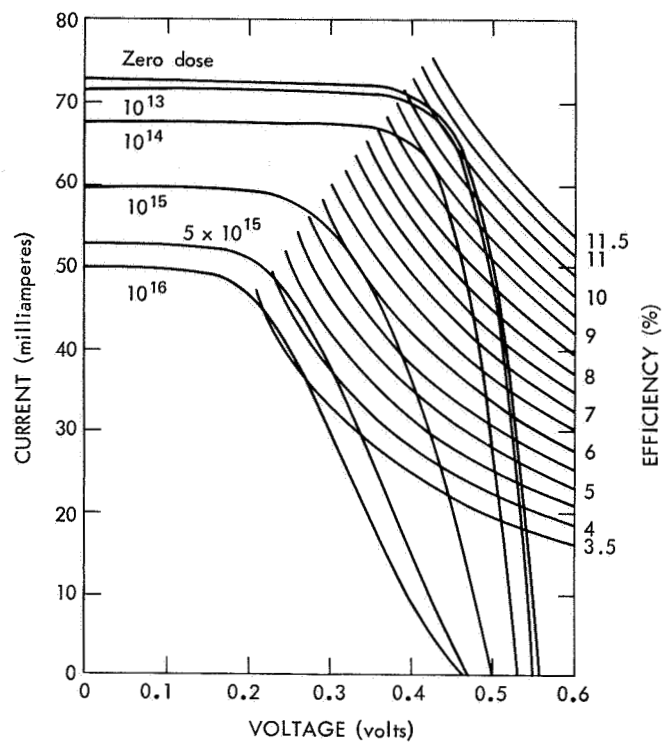


Figure 19—I-V Curves for Siemens Cell G-10 (10 ohm-cm, Boron-Doped).

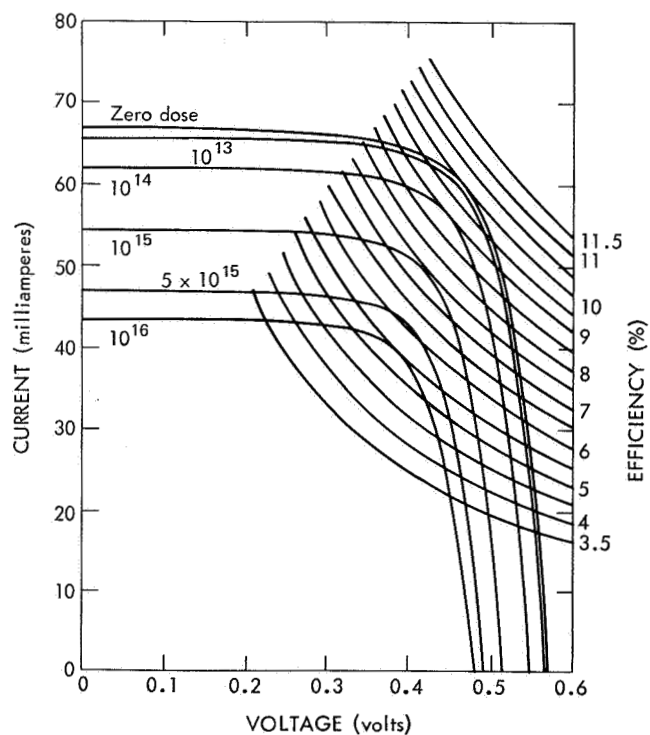


Figure 20—I-V Curves for Heliotek Cell H-9-2 (2 ohm-cm, Boron-Doped).

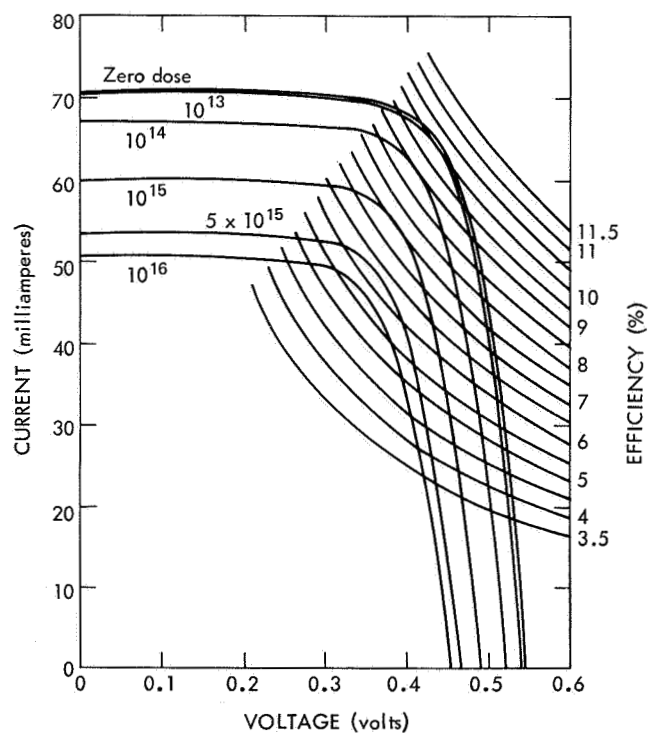


Figure 21—I-V Curves for Heliotek Cell H-10 (10 ohm-cm, Boron-Doped).

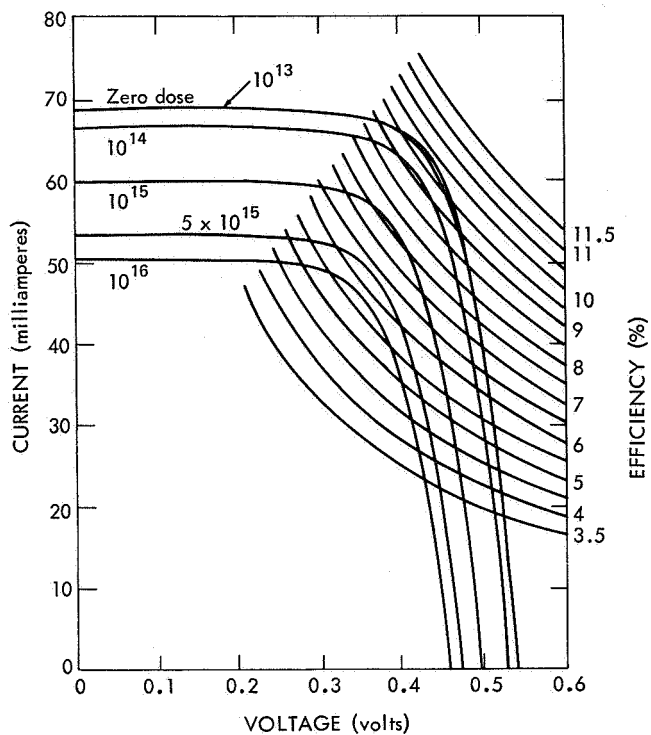


Figure 22—I-V Curves for Ion Physics Cell I-10
(10 ohm-cm, Boron-Doped).

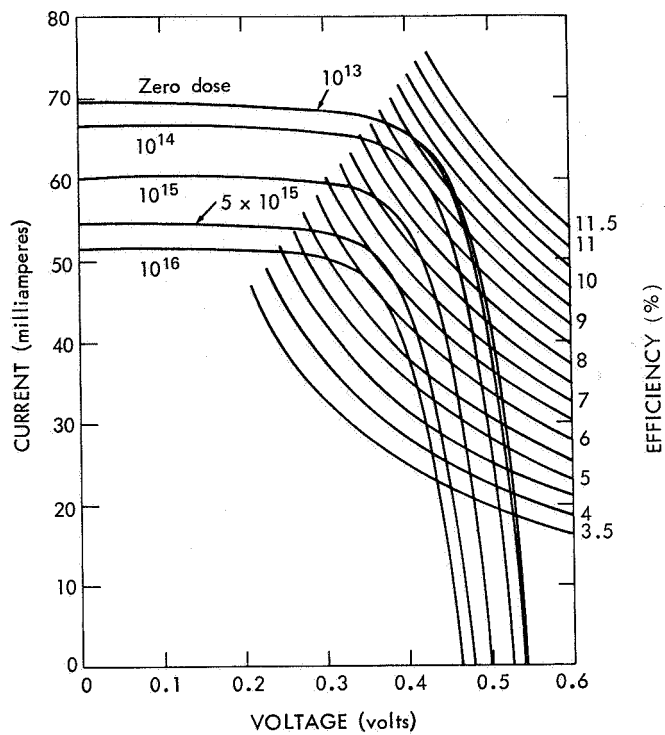


Figure 23—I-V Curves for NASA-Lewis Cell L-10
(10 ohm-cm, Boron-Doped).

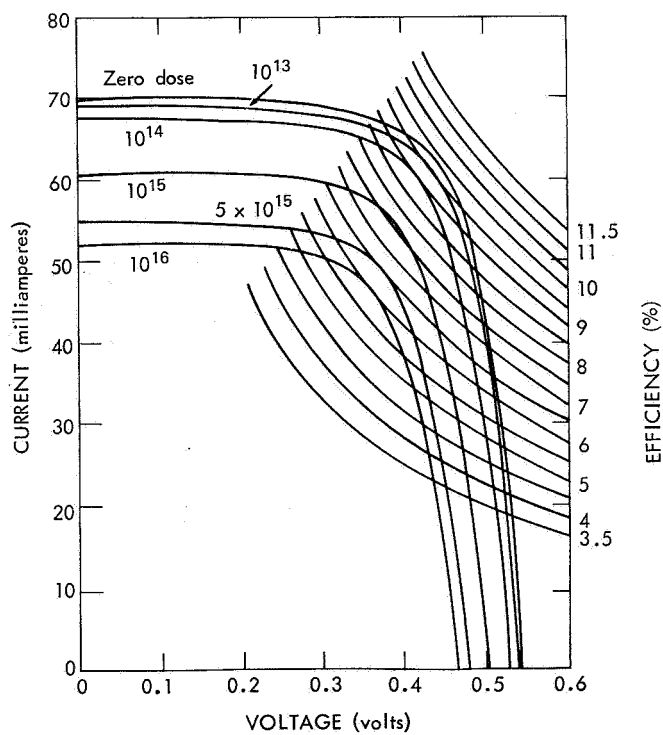


Figure 24—I-V Curves for NASA-Lewis Cell L-10-A
(10 ohm-cm, Aluminum-Doped).

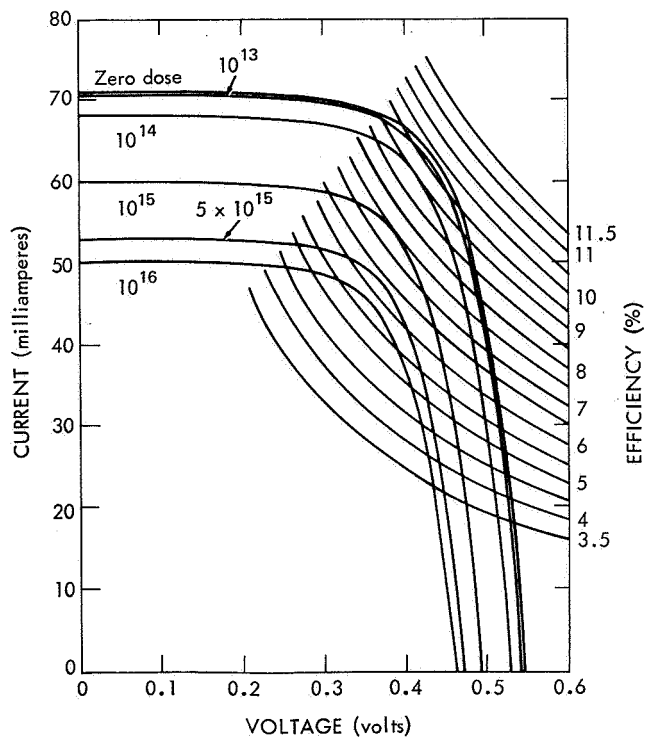


Figure 25—I-V Curves for Texas Instruments Cell T-10
(10 ohm-cm, Boron-Doped).

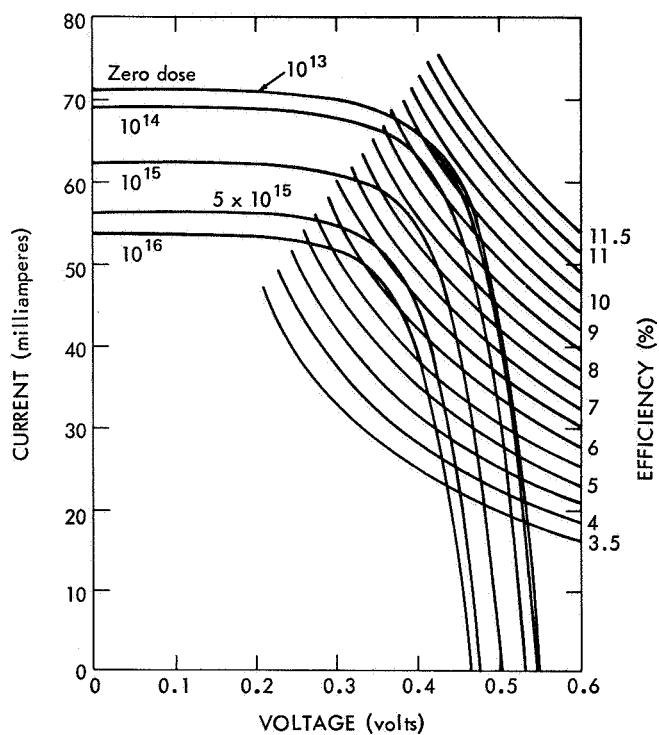


Figure 26—I-V Curves for Texas Instruments Cell T-10-A (10 ohm-cm, Aluminum-Doped).

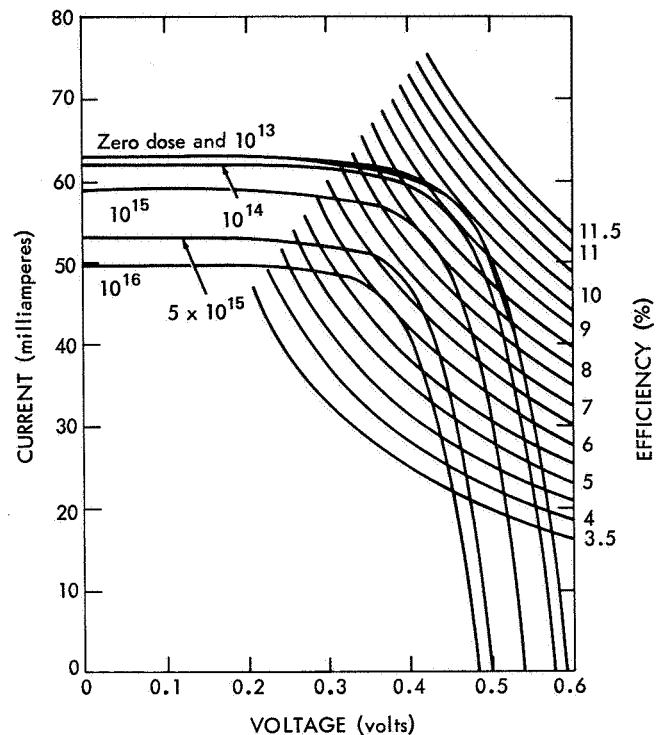


Figure 27—I-V Curves for Westinghouse Cell W-9 (Drift Field).